Structural Engineering and Mechanics, *Vol. 85, No. 2 (2023) 197-206*
https://doi.org/10.12989/sem.2023.85.2.197

Power spectral density method performance in detecting damages by chloride attack on coastal RC bridge

Mehrdad Hadizadeh-Bazaz[a], Ignacio J. Navarro* and Víctor Yepes[b]

Department of Construction Engineering, Institute of Concrete Science and Technology (ICITECH), Universitat Politècnica de València, 46022 Valencia, Spain

(*Received September 24, 2022, Revised December 6, 2022, Accepted December 28, 2022*)

Abstract. The deterioration caused by chloride penetration and carbonation plays a significant role in a concrete structure in a marine environment. The chloride corrosion in some marine concrete structures is invisible but can be dangerous in a sudden collapse. Therefore, as a novelty, this research investigates the ability of a non-destructive damage detection method named the Power Spectral Density (PSD) to diagnose damages caused only by chloride ions in concrete structures. Furthermore, the accuracy of this method in estimating the amount of annual damage caused by chloride in various parts and positions exposed to seawater was investigated. For this purpose, the RC Arosa bridge in Spain, which connects the island to the mainland via seawater, was numerically modeled and analyzed. As the first step, each element's bridge position was calculated, along with the chloride corrosion percentage in the reinforcements. The next step predicted the existence, location, and timing of damage to the entire concrete part of the bridge based on the amount of rebar corrosion each year. The PSD method was used to monitor the annual loss of reinforcement cross-section area, changes in dynamic characteristics such as stiffness and mass, and each year of the bridge structure's life using sensitivity equations and the linear least squares algorithm. This study showed that using different approaches to the PSD method based on rebar chloride corrosion and assuming 10% errors in software analysis can help predict the location and almost exact amount of damage zones over time.

Keywords: Chloride attack; concrete bridge; damage identification; non-destructive technique; Power Spectral Density method (PSD); steel corrosion

1. Introduction

Since the formation of the Sustainable Development Goals in 2015, several scholars have focused on infrastructure upkeep and its implications on the economy, environment, and society (Navarro *et al.* 2018b, Garcia-Segura *et al.* 2018, Navarro *et al.* 2018c). Different deterioration mechanisms, such as chloride ion ingress (Navarro *et al.* 2018a, Zhang *et al.* 2021, Hou *et al.* 2021), carbonation (Sun *et al.* 2020, Ekolu 2020, Zheng *et al.* 2021), or attack by other corrosive agents, such as sulfates, can cause damage to coastal and marine structures. The most dangerous hazard to concrete buildings is chloride-induced corrosion, resulting in excessive economic impacts from their maintenance because of the damage performed in Rc structures (Shekhar et al 2018, Goyal *et al.* 2018). The mechanism of chloride-induced corrosion has been assessed by some researchers in the past (Tang *et al.* 2016, Angst *et al.* 2019). In a coastal RC structure's rebars, the chloride corrosion is done in two levels: initiation and propagation

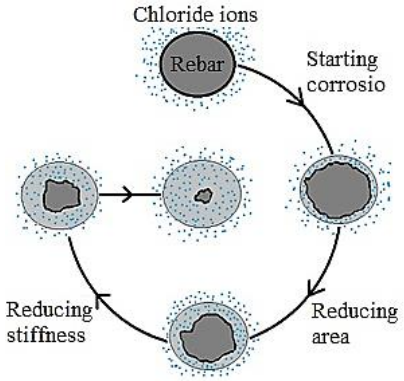

Fig. 1 The process of chloride corrosion in steel rebar

corrosion (Tuutti 1982). When chloride ions arrived at the reinforcement of the concrete structure, they corroded like the process in Fig. 1 over time.

The most challenging aspect of the chloride corrosion mechanism is no visible evidence of damage to the structure. Internal damage in reinforced concrete structures can be detected using destructive or non-destructive methods. Destructive methods are dependent on models that often involve removing structure samples to assess the damage. Nevertheless, non-destructive methods are independent models that can identify damage to a numerical model in software without affecting the structure (Rathod and Gupta 2019). These non-destructive damage detection

*Corresponding author, Ph.D.
E-mail: ignamar1@cam.upv.es
[a]Ph.D. Student
E-mail: M.hadizadehbazaz@doctor.upv.es
[b]Professor
E-mail: vyepesp@cst.upv.es

ISSN: 1225-4568 (Print), 1598-6217 (Online)

methods can be monitored according to signal-based techniques. Due to modern and intelligent computers and sensors, signal-based approaches for health monitoring have increased in structures (Yang *et al.* 2021). Some signal-based approaches include time-domain (Aloisio *et al.* 2020, Yu *et al.* 2021), frequency-domain (Pérez *et al.* 2021, Ronchei *et al.* 2021), and time-frequency domain (Wu *et al.* 2022, Tran *et al.* 2020). These methods reveal structural systems' dynamic characteristics (Najafabadi *et al.* 2017) and thus when relevant damage has occurred by different causes, such as chloride corrosion. In summary, time-domain methods frequently use for stochastic processes (Seyedpoor *et al.* 2011). The frequency-domain methods can produce many responses and data from frequency points by specifying model updating equations (Arora 2011). Some dynamic frequency-domain methods include: Natural Frequency (Wang 2021, Khan *et al.* 2020), Power Spectral Density Function (Zheng *et al.* 2015, Pedram *et al.* 2017, Gao *et al.* 2021), Frequency Response Function (Rahmatalla *et al.* 2012, Niu 2020), Mode Shape (Hou *et al.* 2018, Xu *et al.* 2020), Modal Strain Energy (Arefi and Gholizad 2020, Khosravan *et al.* 2021), and Modal Curvatures (Dessi and Camerlengo 2015, Ganguli 2020, Pooya and Massumi 2021). Finally, the data in the time-frequency domain is derived from the observed signal frequency over time (Aquino *et al.* 2021). Some time-frequency approaches for modal identification include Wavelet Transform (WT) (Silik *et al.* 2021), Blind Source Separation (BSS) (Li *et al.* 2020), and also Empirical Mode Decomposition (EMD) (Barbosh *et al.* 2020).

The Power Spectral Density (PSD) is a method based on frequency-domain techniques that uses a periodic or random signal's frequency response. The frequency response defines the mean power distribution. This method uses a sensitive nonlinear function of structural parameters to define a second-order transfer function (Nilsson and Liu 2015). In recent years, researchers in different fields have investigated the reliability of the PSD method for identifying various damage types. Bayat *et al.* (2019) tested a novel technique based on the PSD function and the Least Square Distance approach to identify deterioration in bridge concrete piers. Gunawan (2019) assessed the reliability of the PSD method on seven lumped masses (1 kg) that were connected by eight similar linear elastic springs. Hadizadeh-Bazaz *et al.* (2022) Compared the performance of Power Spectral Density (PSD) by Frequency Response Function in a steel bridge structure.

This study evaluated the PSD method's performance to identify damages by chloride attack on the RC Arosa bridge in Spain with columns located and contacting seawater. The damage on the bridge was analyzed according to changes in dynamic parameters and decreasing rebar cross-section areas during chloride corrosion time by new approaches using the PSD method as a frequency-domain technique by using sensitivity equations and the linear least square methodology. For years, some researchers have considered optimization and optimization methods with different methods and goals (Carbonell *et al.* 2011, Penadés-Plà *et al.* 2019). For this reason, this research result can help optimize maintenance costs and reduce life cycle costs (LCC) and even other life cycle impacts (environmental and social) as

Fig. 2 The location map of the Arosa bridge in Spain

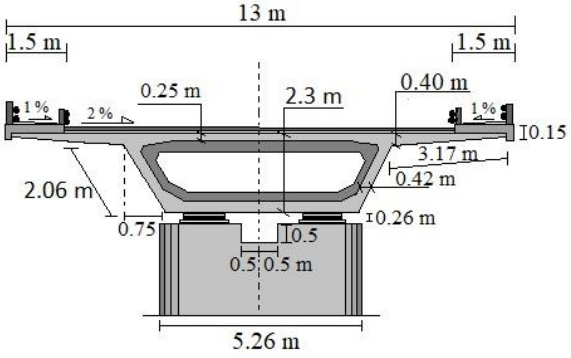

Fig. 3 Arosa's concrete bridge in cross-section

an accurate method. In order to avoid wasting time and money, it is essential to know the specific location of damage to buildings such as bridges.

2. Methods and materials

This study identifies the RC bridge damaged by chloride corrosion in steel reinforcements analyzed over the structure life by combining two-step methods. The initial step was to determine the steel components' service life using Fick's second chloride diffusion equation. Then, in the second step, the existence, quantity, and location of chloride damage to the concrete caused by steel reinforcements' chloride corrosion were investigated according to the PSD method by measuring the frequency response function and monitoring changes in dynamic parameters. The bridge structural model description includes diameters and materials and is explained as follows.

2.1 Model description

This concrete bridge is called the Arosa Bridge, and it is located in Galicia, Spain (see Fig. 2). This bridge is 1980 m long and has 40 spans (the first and end spans are 40 m, and the other 38 intermediate spans are 50 m). This construction's geometry and durability parameters were based on data from the literature (González *et al.* 2013, Pérez-Fadón 1985, Pérez-Fadón 1986).

The concrete bridge deck is a single box girder. As indicated in Fig. 3, the bridge deck is 13 m wide and 2.30

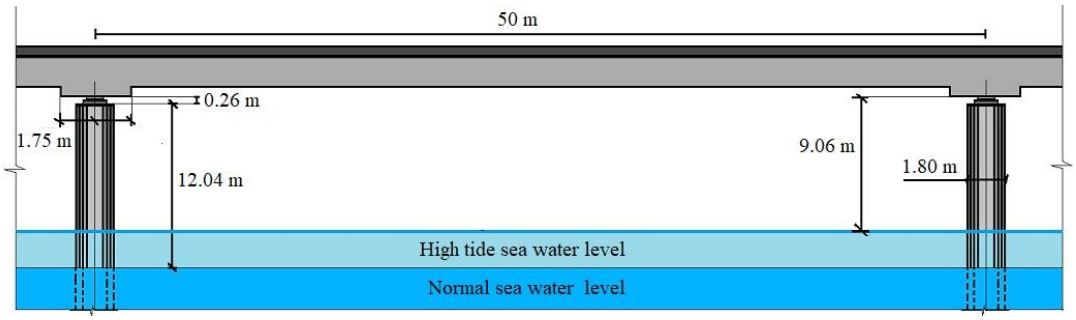

Fig. 4 The geometry of a span of the bridge

Table 1 The Arosa structure's concrete mixtures and mechanical parameters

Properties (Units)	Water (l/m^3)	Cement (kg/m^3)	Gravel (kg/m^3)	Sand (kg/m^3)	f_{cm} (MPa)	E_c (GPa)	w/c (%)
Amount	218.5	485.6	926.7	827.9	40	29	0.45

meters high. Two pedestrian walkways run along the deck's sides. Each walkway is 1.5 m wide.

The column dimensions are 5.26 m wide and 1.80 m thick. Under normal circumstances, the bridge deck is about 12 m above the sea and 9.6 m during high tide (see Fig. 4).

The concrete cover on the reinforcements for the deck, 35 mm, and for the columns, 45 mm was considered. The reinforcing steel quantity is 100 kg/m^3 of concrete. Assumed concrete mixes and mechanical parameters for the bridge are in Table 1 (Pérez-Fadón 1985).

According to the Table1, the concrete mix for the bridge has a water-to-cement ratio (w/c) of 0.45 and contains 485 kg/m^3 of cement.

2.2 Chloride damage prediction methods for the rebars of RC structure

Most metals are vulnerable and susceptible to natural and manufactured influences, particularly in coastal areas where chloride ions cause corrosion. Corrosion is common in reinforced concrete structures like bridges and concrete marine structures. According to the deterioration model proposed by Tuutti (1982), these commissions and damages by chloride in rebars of a concrete structure have some service life levels, such as the initiation and propagation phases depicted in Fig. 5. (Tuutti 1982, Hájková and Šmilauer 2018).

As illustrated in Fig. 5, chloride corrosion begins in the Initiation corrosion Phase. At the initiation phase, there are chlorides, but at an amount that is less than the chloride threshold (that means it is not enough to start the corrosion process). The propagation phase of chloride ion activity includes some levels, such as commencing corrosion, cracking on the concrete cover, the serviceability limit state, and the last level is the ultimate limit state (Zhang *et al.* 2019).

According to the fellow equation, estimating the total time to chloride corrosion (t_l) as the service life of reinforcements of the bridge structure by summing the initiation and propagation phases together (Spanish Ministry of Public Works 2008).

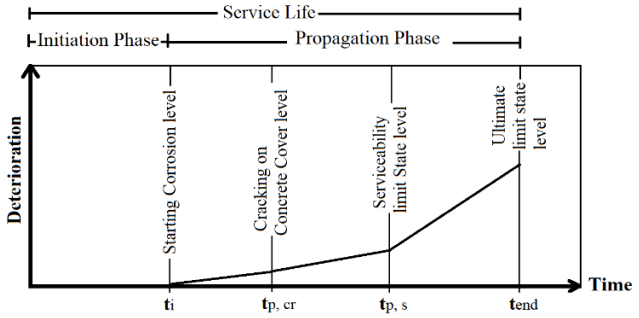

Fig. 5 The service life of rebars and chloride corrosion levels in RC structures

$$t_l = t_i + t_p \tag{1}$$

Where t_i is the corrosion initiation period, defined as the time, it is the time for the chlorides to reach the rebars and a high enough concentration to start corrosion (chloride threshold, dependent on the steel properties and to some extent on the concrete properties). Also, t_p is the corrosion propagation period time to spread through a structural member until it deteriorates significantly (Spanish Ministry of Public Works 2008).

2.2.1 Initiation chloride corrosion Phase (t_i)

According to Fick's second law of chloride diffusion mathematically model and the Spanish concrete design code, the initiation of chloride corrosion is the time to reach a particular concentration to befall from the surface of concrete covers through the following (Spanish Ministry of Public Works 2008, Khan *et al.* 2017).

$$C(x,t) = C_s \cdot \left(1 - erf\left(\frac{x}{2\sqrt{D_{0,x} \cdot (\frac{t_0}{t})^{\alpha} \cdot t}}\right)\right) \tag{2}$$

Where $C(x,t)$ is the chloride concentration (wt%/binder) at the concrete cover depth x (mm) and during time t (years). C_s is the surface chloride concentration (wt%/binder) at the concrete cover surface. The approximate value of C_s can be extracted according to Table 2. The *erf*(.) is the Gauss error function. α is the age factor considered 0.5, as the Spanish concrete design code. t_0, as the reference time is considered 28 days change the unit to year (t_0=0.0767) and also D_0, is the non-steady-state chloride diffusion coefficient (mm^2/years) at the age t_0 can be obtained from Table 3. (Spanish Ministry of Public

Table 2 The chloride concentration at the concretes surface in the marine environment (Spanish Ministry of Public Works 2008)

Marine exposure class	Aerial (IIIa)		Submerged (IIIb)	In Tidal Zone (IIIc)
Distance from the coast	Up to 500 m	500-5000 m	Any	-
C_s (% of concrete weight)	0.14	0.07	0.72	0.50

Table 3 The coefficients D_0 ($\times 10^{-12}$m^2/s) (Spanish Ministry of Public Works 2008)

Type of cement	*w/c*=0.40	*w/c*=0.45	*w/c*=0.50	*w/c*=0.55	*w/c*=0.60
CEM I	8.9	10.0	15.8	19.7	25.0
CEM II/A-V	5.6	6.9	9.0	10.9	14.9
CEM III	1.4	1.9	2.8	3.0	3.4

Works 2008, Crank 2004).

In this investigation, according to the Arosa bridge situation and distance from the salt water, the amount of the *Cs* was considered 0.14 for the deck and upside of the bridge columns and 0.72 and 0.50 for the submerged and in tidal zone sections of the columns, respectively. Furthermore, the coefficients D_0 according to the type of cement and w/c were assumed to be 10. However, the chloride transport time (t) can calculate using the inverse of Eq. (2) as Eq. (3).

$$t = \frac{x^2}{4D}\left[erf^{-1}\left(\frac{C_s - C(x,t)}{C(x,t)}\right)\right]^{-2} \quad (3)$$

Where the D is the chloride diffusion coefficient, which varies with the age of the concrete ($D=D(t_0)(t_0/t)^n$). Additionally, when $C(x,t)$ reached threshold concentration C_t and also, if $C(x,t)=C_t$ then the Initiation Period of chloride diffusion (t_i) determined as follows at Eq. (4) (Spanish Ministry of Public Works 2008, Khan *et al.* 2017, Sobhani ans Ramezanianpour 2007, Bendat *et al.* 1980).

$$t_i = \frac{x^2}{4D}\left[erf^{-1}\left(\frac{C_s - C_t}{C_s}\right)\right]^{-2} \quad (4)$$

Moreover, the critical chloride concentration value under normal conditions as the mean value can consider 0.6% of the cement weight. When the chloride concentration (C) is greater than or equal to the value of the critical chloride concentration (C_{th}), the initial corrosion time of the steel bar equals the transport time (t), indicating that corrosion and damage to the rebars begin at this time. In contrast, less than this value means that damage in the reinforcements has not started (Spanish Ministry of Public Works 2008, Navarro *et al.* 2019).

2.2.2 Propagation chloride corrosion phase (t_p)

This stage begins after the Initiation stage of chloride diffusion when chloride ions on the surface of the inner rebars start to corrode steel reinforcements. Chloride corrosion cause reduces the cross-sectional area and stiffness of the steel bars over the years. The Spanish concrete design code (Spanish Ministry of Public Works 2008) gives the following equation for calculating this time

Table 4 The Chloride corrosion rate depended on the Marine exposure class (Spanish Ministry of Public Works 2008)

Marine exposure class	Aerial (IIIa)	Submerged (IIIb)	In Tidal Zone (IIIc)
V_{corr} (μm/year)	20	4	50

$$t_p = \frac{80}{\phi}\frac{d}{V_{corr}} \quad (5)$$

Where t_p is the propagation time in years. Also, d is concrete cover thickness, the ϕ is the reinforcement diameter, and V_{corr} is the corrosion rate. The approximate value can be obtained from Table 4.

To calculate the propagation time, the approximate speed of chloride corrosion on rebars, V_{corr}, depends on the situation of the structure elements considered in Table 4. In addition, the concrete cover (d) for the deck was considered 35 mm and 45 mm for columns with a rebar diameter of 32 mm in the concrete Arosa bridge.

Overall, according to the initiation and the propagation levels for chloride corrosion of reinforcements of an RC marine or coastal structure, the damage induced by corrosion to the reinforcement can be calculated as a percentage using the equation below

$$Dam_{steel}(t) = \frac{t - t_i}{t_p} \times 100 \quad (6)$$

In Eq. (6), Dam_{steel} is the damage percentage of reinforcement by chloride corrosion for every year (t) during propagation t_p.

The damage percentage was analyzed for the RC bridge's deck and columns according to the different situations and marine exposure classes such as the Aerial, Submerged, and In Tidal Zone. Moreover, the changes in stiffness and loss of cross-section area of reinforcement for identifying damages on the concrete of the RC structure were obtained according to this chloride corrosion damaged percentage during structure life.

2.3 Damage detection methods for the total of the RC bridge

In this annalize, the PSD method, which is non-destructive and dynamic, was used to identify these damages in the concrete part according to the damages percentage of corroded rebars by chloride. For this purpose, changes in the dynamic characteristics of each year and situation due to decreasing cross-sectional areas and rebar stiffness were considered in this investigation.

2.3.1 Power spectral density method

The PSD is vibration and signal-based method; therefore, this method was obtained according to the frequency response function (FRF) method as following equations (Hadizadeh-Bazaz *et al.* 2022, Zheng *et al.* 2015, Pedram *et al.* 2017). The transfer function is defined as, Eq. (7)

$$H(\omega) = (K - \omega^2 M + i\omega C)^{-1} \quad (7)$$

K, M, and C are the matrices of stiffness, mass, and

damping, respectively; ω is the frequency and $i=\sqrt{-1}$. The PSD equation of structural response simplifies as Eq. (8)

$$S_{XX}(\omega) = H^*(\omega)S_{FF}(\omega)H^T(\omega) \quad (8)$$

Where S_{FF} is the PSD inputs matrix at all of the active Degree Of Freedom (DOF); $H^*(\omega)$ is the complex conjugate of a transfer function. As shown in Eq. (8), the power spectral density is a second-order function of the FRF, which can be a highly nonlinear response to structural elements.

To model updating based on the sensitivity equation, Eq. (8) to expand as the following format by considering (K-ω^2M+$i\omega C$=$Z(\omega)$) in the below equation

$$Z^*(\omega)S_{XX}(\omega) = S_{FF}(\omega)H^T(\omega) \quad (9)$$

where $Z(\omega)$ is the impedance matrix and the transfer function inverse. Eq. (9) for the damaged structure due to chloride corrosion to the reinforcement of structure is as follows

$$[Z^*(\omega) + \Delta Z^*(\omega)][S_{XX}(\omega) + \Delta S_{XX}] = S_{FF}(\omega)[H^T(\omega) + \Delta H^T(\omega)] \quad (10)$$

According to Eqs. (10)-(9), the power spectral density function equation is changed by considering ($\Delta Z(\omega)$=ΔK-$\omega^2\Delta M$+$i\omega\Delta C$) and ($H_D(\omega)$=$[Z(\omega)$+$\Delta Z(\omega)]^{-1}$). Where $H_D(w)$ is the FRF of damaged RC structure during rebars damaged by chloride corrosion every year by Eq. (6), therefore, Eq. (10) can be rewritten as Eq. (11).

$$\Delta S_{XX}(\omega) = H_D^*(\omega)S_{FF}(\omega)\Delta H^T(\omega) - H_D^*(\omega)\Delta Z^*(\omega)S_{XX}(\omega) \quad (11)$$

H^*_D is the complex conjugate of the damaged RC structure transfer function during reinforcement chloride corrosion according to Eq. (6).

As the expression of the exact ΔH presented by Esfandiari *et al.* (2009) in Eq. (12)

$$\Delta H(\omega) = -H_D(\omega)(\Delta K - \omega^2\Delta M + i\omega C)H^T(\omega) \quad (12)$$

Eq. (11) can be rewritten by using Eqs. (8)-(12) as follows

$$\Delta S_{XX}(\omega) = -H_D^*(\omega)S_{FF}(\omega)H_D(\omega)(\Delta Z(\omega))H^T(\omega) - H_D^*(\omega)(\Delta Z^*(\omega))H^*(\omega)S_{FF}(\omega)H^T(\omega) \quad (13)$$

To identify the damages caused by corrosion on the reinforcement bars and its effect on the structural behavior of the system, the stiffness of each reinforced concrete element is modified in proportion to the corrosion damage calculated for each time for the rebars. The following is a list of the modifications that have been made to the stiffness, mass, and damping matrices as a result of changes in dimensionless structural parameters

$$\begin{cases} \Delta K = \sum_{n=1}^{ne} K_n \Delta P_n^K \\ \Delta M = \sum_{n=1}^{ne} M_n \Delta P_n^M \\ \Delta C = \sum_{n=1}^{ne} C_n \Delta P_n^C \end{cases} \quad (14)$$

Where K_n, M_n, and C_n are the stage of stiffness, mass, and damping matrices of the structural elements of a structure, ΔP_n^K, ΔP_n^M, and ΔP_n^C indicate that structural parameter changes are between -1 and 1. The monitoring of changes in stiffness and mass and damping of the structure due to possible damage to a structure through the PSD damage identification method during the lifetime of this structure has been calculated using Eq. (14), then according to Eq. (13) and considering ($\Delta Z(\omega)$=ΔK-$\omega^2\Delta M$+$i\omega\Delta C$). So depending on changes in dynamic characters because of damage causes such as chloride corrosion damages, the sensitivity matrices assigned to the n^{th} parameter of structure for obtaining the unknown stiffness, mass, and damping ratios is as follows

$$\begin{cases} S^K = -H_D^*(\omega)S_{FF}(\omega)H_D(\omega)K_nH^T(\omega) \\ \quad -H_D^*(\omega)K_nH(w)S_{FF}(\omega)H^T(\omega) \\ S^M = \omega^2(H_D^*(\omega)S_{FF}(\omega)H_D(\omega)M_nH^T(\omega) \\ \quad +H_D^*(\omega)M_nH(w)S_{FF}(\omega)H^T(\omega) \\ S^C = i\omega(-H_D^*(\omega)S_{FF}(\omega)H_D(\omega)C_nH^T(\omega) \\ \quad +H_D^*(\omega)C_nH(w)S_{FF}(\omega)H^T(\omega) \end{cases} \quad (15)$$

The final equation of PSD for calculating changes in dynamic properties parameter during damage repeat for every year can predict from Eq. (16)

$$\Delta S_{xx} = S^K\Delta p_K + S^M\Delta p_M + S^C\Delta p_C \quad (16)$$

The sensitivity Eq. (16), according to the changes in the structural parameters, is linear. To obtain analyses according to the nonlinear optimization, changes in dynamic characters depend on the initial damage analysis in each structure element during the time monitoring and obtained. In addition, a balanced focus on these elements reduces estimate errors in finite element method model updating with the appropriate solution using standard least squares. In this study, the identification of damages for different parts using the PSD method and through the sensitivity equation with consideration for the time for each year of the structure's life is presented in the form of an updated model according to the scenarios of predicting the corrosion damage of rebars by chloride ions evaluated and investigated the reinforced concrete structure.

2.3.2 Numerical model evaluation

With the development of computers and the increasing their speed and performance, the use of non-destructive and independent models according to numerical models of structures to identify damage is attractive to many engineers and researchers. In this study, the performance of the PSD method, which is a vibration and signal-based method, was used to look for damage caused by chloride ions on a numerical model of a concrete bridge in a coastal area.

For the health monitoring of the bridge structure each year from the beginning corrosion time to the end corrosion time of the reinforced concrete bridge reinforcement, some points and sensors were considered for the numerical model of the bridge at specific distances from each other. Then, as in Fig. 6, they were renumbered from 1 to 183 on the deck and columns of these selected spans. These three spans in the middle of the bridge were selected from forty spans because these parts could be the most chloride attack. However, the bridge was analyzed in software with almost the same signal information and conditions all over the bridge.

Fig. 6 shows the three spans from the middle of the total numerical model of the Arosa bridge. Numbering starts from 1 to 155 for the bridge deck and from 156 to 183 for

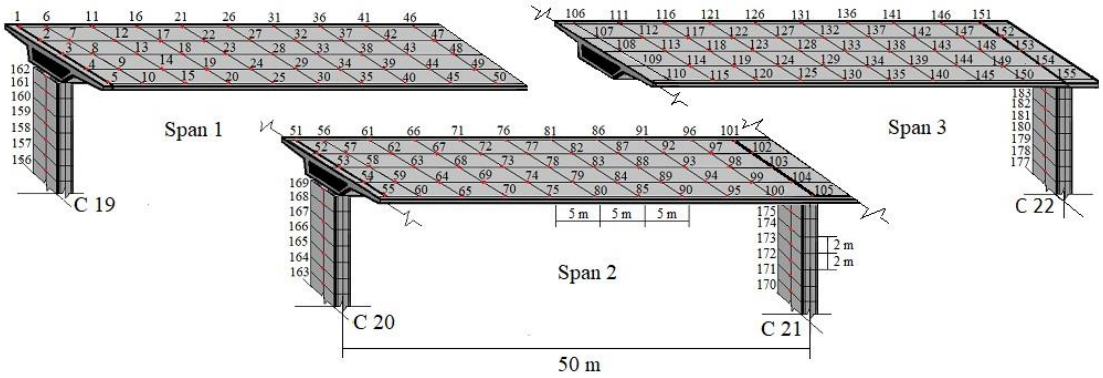

Fig. 6 Numbering and dividing points in the three spans selected of the Arosa bridge

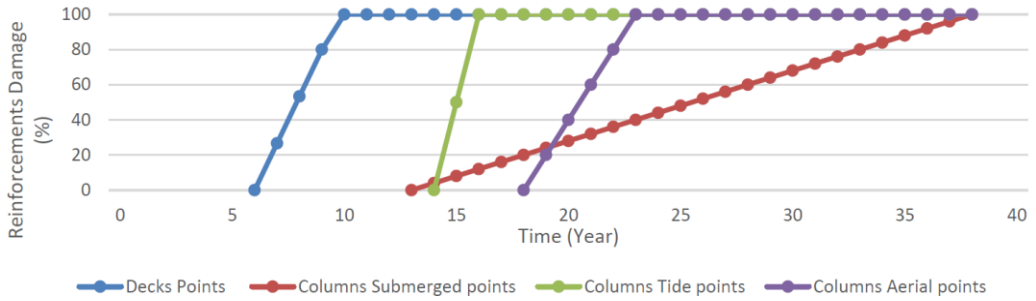

Fig. 7 The deterioration of the reinforcements of the bridge according to chloride corrosion attacks every year for different locations

columns C19 to C22.

To monitor the amount of damage at each location of the bridge sections for each year, consider some points as simulation points and some other points as measurement points. The position and situation of these excitations and measurement points for annual test monitoring and analysis were assumed to be fixed every year analyzed. For this analysis assessment, some points at the center of each span over the supports and points at the middle of the columns were selected as the simulation points, and the rest were selected as the measurement points.

Therefore, in these three spans of the bridge for the deck, points 3, 28, 53, 78, 103, 128, and 153 were selected as stimulation points, and also, for columns points 159, 166, 173, and 180 were considered as stimulation points. Moreover, In this numerical investigation, the performance of chloride ions in the destruction of any part of this coastal concrete bridge assumed 10% noise and errors. Identifying the location and extent of damage to the bridge due to corrosion of the internal rebars of the reinforced concrete bridge was done as a new approach.

Overall, in this study, the damage caused to the rebars of each element of the concrete coastal bridge was identified according to the location and the distance of each part to the seawater, which can have an effect on the rate of corrosion and damage of the rebars and metal parts of the structure, and with using the equations related to the service life and the corrosion rate of the reinforcements by chloride, which was mentioned in the previous sections, predicted the amount of damage to the rebars of each part and area of the bridge, then according to these damages that the corrosion by chloride causes a reduction the diameter and stiffness of reinforcements and rebars can be calculated and model updating for every year. By taking into consideration, the changes in dynamic characteristics, the percentage of the damages was determined for different parts of the bridge structure depending on the situation of each element (including submerged, in tide zone, and dry parts such as deck and the upper parts of columns bridge) in each year compared to the previous year amount of damages by considering a constant location and frequency interval from the excitation points for each year in software. These changes in the characteristics of the structure are caused by the damage caused by chloride ions, which cause changes in the quantity of FRF data in each year from the failure of the structure to the undamaged structure (after 28 days from the construction of the structure) is different. Finally, according to the difference, the frequency response has been monitored and analyzed through the PSD equation via software in the numerical model of the bridge.

To evaluate the performance of the PSD method in detecting damage caused by the presence and activity of chloride ions was analyzed according to MATLAB software and finite element-based by Open Sees software.

3. Results

The damage identified to the bridge structure caused by the chloride attack was analyzed as the first step damage in the reinforcements according to each section's position to the seawater. So damages prediction for reinforcements en every year of bridge life from beginning to end chloride corrosion of rebars shows in Fig. 7.

The results in Fig. 7 show the monitoring of the damage prediction of rebars that cause a loss in the area section of

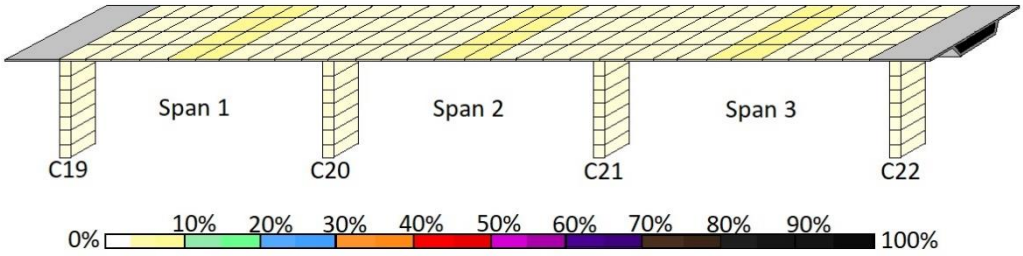

Fig. 8 Damage location and percentage due to chloride attack in the 5th year of the bridge life

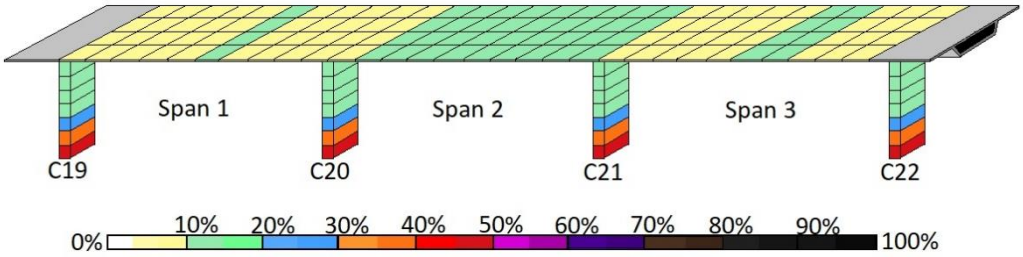

Fig. 9 Damage location and percentage due to chloride attack in the 10th year of the bridge life

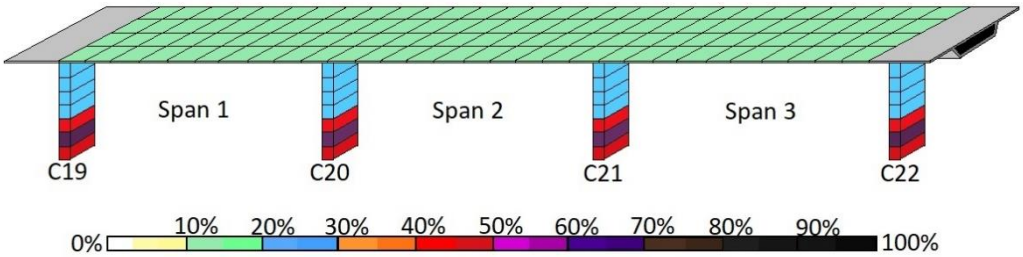

Fig. 10 Damage location and percentage due to chloride attack in the 15th year of the bridge life

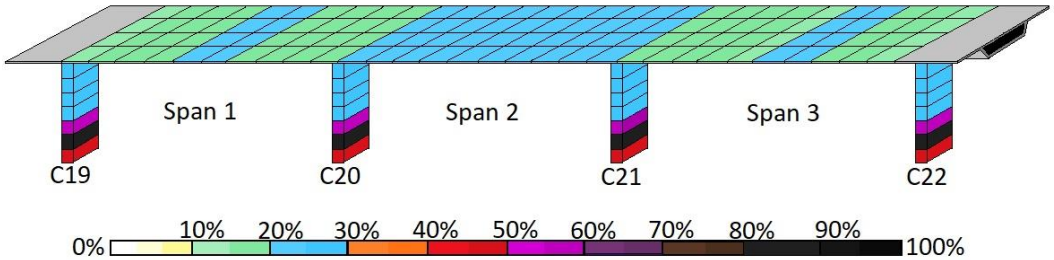

Fig. 11 Damage location and percentage due to chloride attack in the 33rd year of the bridge life

reinforcement at each measurement and simulation point of the numerical Arosa bridge model (see Fig. 6). The damages in reinforcements of the decks' points, including points 1 to 155, started only six years after the bridge was built. 26.67, 53.33, and 80 percent were corroded and damaged in the seventh, eighth, and ninth years. On the other hand, the chloride corrosion damages rebars for every part, and the element of columns are different. This kind of damage percentage for the submerged point zone (area sections between points 156-157, 163-164, 170-171, 177-178) began from the thirteenth year, and damages regularly increased by about 4 percent every year until the thirty-eighth years. In addition, the damage amount for reinforcements in the tide points zone (area sections between points 157-158, 164-165, 171-172, 178-179) started from the fourteenth year of the bridge's life. After one year in the fifteenth year damaged, these reinforcements increased dramatically by about 50 percent, and in the sixteenth year, they completely corroded. Finally, the columns' rebars in the aerial point zone (the area sections between points 158-162, 165-169, 172-176, 179-183) began in the eighteenth year until the twenty-three year with increasing damages of about 20 percent in every year after beginning corrosion.

However, the amount and location of corrosion along one RC bridge's structural element can differ according to various reasons caused during or after construction. The amount of damage to each element of the reinforced concrete bridge has been obtained using the PSD technique presented above. Moreover, quantified damages in the bridge are obtained by average damage percentages for every area between four measurement points in different

parts of the concrete bridge structure spans during the chloride corrosion in reinforcements. The obtained damage results for each element are presented below for different time horizons (Figs. 8-11).

The above figures show the damage percentage in different concrete parts according to the beginning corrosion time in the reinforcements of each zone of the RC Arosa bridge in terms of distance from seawater and chloride ions. According to Figs. 8-11, the amount and location of concrete structural damages predicted by the PSD-based method from the fifth year by starting rebars corrosion at the deck and until end reinforcements corrosion in 33th years of the bridge life at the submerged zone of columns of the bridge. The damage in the deck points (1-155) was less than ten percent in the 5th year and between ten and thirty percent in the 33rd year. Nevertheless, damages situations in all parts of columns are different. The damages percentage for areas between measurement points in the submerged zone (points 156, 157, 163, 164, 170, 171, 177and 178) that sections are sink in seawater in the 5th year (Fig. 8) are less than five percent. After five years, in the 10th year, about fifty percent of the reinforcement was corroded (Fig. 7), and the concrete of these areas was damaged by about forty percent. In the 33rd year, the bridge life damage percentage increased by about fifty percent.

On the other hand, the quantified damages in the points located in the tide zone (points 157, 156, 164, 165, 171, 172, 178, and 179) between the 5th year to the 33rd year (Figs. 8-11) are less than five percent in 5th year and about forty percent in 10th year and about sixty percent in the 15th year and finally in the 33rd year these parts damaged more than seventy percent. Furthermore, the damage percentage for the aerial columns points zone in the 10th year of the bridge life (Fig. 9) is less than twenty percent. However, by starting rebars, corrosion in upside columns areas in the 15th year, the concrete damage is increased to about thirty percent in 15th and 33rd years that the chloride corrosion almost was done as Fig. 7.

4. Conclusions

Because the performance and accuracy of various non-destructive and dynamic methods on the numerical model for various factors are increasing over time thanks to modern computers and sensors for the maintenance of important structures such as bridges, and furthermore because all methods for damage detection for different damage causes in different kinds of structures and environments have not been assessed. So research into these methods for various structures, the environment, and the factors that cause damage is critical. Considering these issues, this study has specifically evaluated the feasibility of the PSD method as a damage detection approach with a different approach to detect damage caused only by chloride ions in concrete buildings. On the other hand, the accuracy and effectiveness of this method in detecting this type of damage by chloride ions in every part of these coastal structures during their lifetime have been discussed.

The result of this research helps a lot in reducing the costs of repairing and maintaining the bridge structure, preventing sudden damage and collapse of this structure, and thus maintaining the safety of human lives. The results of analysis on the numerical model on software by PSD methods showed that naturally, corrosion by chloride was different for every situation and bridge element's distance from the seawater. Also, the speed and acceleration of corrosion of bars in every part were not the same, affecting damages to other parts. Over time, the damage increased slowly and slowly in the deck and upper columns that were not in contact with seawater and chloride ions. Also, parts of the pillar bases submerged in seawater have seen less speed over time than other parts of the bridge, which can be due to a lack of oxygen and air, which indicates the presence of too much oxygen in increasing the rate of failure. The chloride device is effective. However, the damage to the points and parts of the columns in the tidal range is severe, dangerous, and worrying because, only after a few years and in a short time, this area of the columns was severely damaged by chloride attack.

As Summarize the results of used PSD method to identify chloride damages on the concrete part of the RC bridge and reinforcement chloride corrosion, the below conclusions can be obtained:

- The PSD method's analysis showed that this method has high accuracy in detecting the location of internal and external concrete damages caused by reinforcement chloride corrosion in a coastal RC structure.
- One of the significant issues with testing on an experimental model is the inability to determine the internal condition and amount of damage to each part of a concrete structure, especially inside a coastal concrete bridge. While using the numerical model and by PSD method, determining and identifying the location and quantified damage during the structure's life was easier, cheap, and any destructive to structure to make information from the inner part of the structure.
- The PSD method for identifying damages due to chloride corrosion was efficient and reliable in lower frequency ranges between the stimulation points and the measurement points at software, which could be an advantage for small structures.
- In general, bearings and dampers control nonlinear behavior between columns and decks, affecting the PSD method's detection of concrete damages due to chloride corrosion on the entire bridge.
- One of the drawbacks of frequency-domain methods like the PSD is locating the measuring and excitation points, which requires trial and error to locate these points, especially for large and critical structures like bridges. Because improper stimulation and measuring points can affect the final results, this field requires skilled experts.
- Numbers of the excitation points and measuring points could help bridges and structures detect damage more accurately, but increasing these sensors requires powerful and fast computers, which is a significant disadvantage of the PSD method for analysis in the numerical model of the bridge.

Although chloride-induced damage to coastal RC structures is particularly harmful, it generally starts on the inside of the structure, which causes significant inner and

invisible damage. If these damages are not identified and repaired on time, they could even suddenly collapse some parts of the bridge. This study showed that this method has acceptable results in detecting the amount of damage caused by chloride corrosion of rebars and the activity of chloride ions in each year of bridge life. Thus, using the FE approach on numerical models, non-destructive health monitoring, and damage detection can save money and human lives by on-time repair through the PSD methods for damages by chloride ions.

Acknowledgments

Grant PID2020-117056RB-I00 funded by MCIN/AEI/ 10.13039/501100011033 and by "ERDF A way of making Europe".

References

Aloisio, A., Alaggio, R. and Fragiacomo, M. (2020), "Time-domain identification of the elastic modulus of simply supported box girders under moving loads: Method and full-scale validation", *Eng. Struct.*, **215**, 110619. https://doi.org/10.1016/j.engstruct.2020.110619.

Angst, U.M., Geiker, M.R., Alonso, M.C., Polder, R., Isgor, O.B., Elsener, B., ... & Sagüés, A. (2019), "The effect of the steel-concrete interface on chloride-induced corrosion initiation in concrete: A critical review by RILEM TC 262-SCI", *Mater. Struct.*, **52**(4), 1-25. https://doi.org/10.1617/s11527-019-1387-0.

Aquino, R.E., Barbosh, M. and Sadhu, A. (2021), "Comparison of time-domain and time-frequency-domain system identification methods on tall building data with noise", *Dyn. Civil Struct.*, **2**, 179-184. https://doi.org/10.1007/978-3-030-47634-2_20.

Arefi, S.L. and Gholizad, A. (2020), "Damage identification of structures by reduction of dynamic matrices using the modified modal strain energy method", *Struct. Monit. Maint.*, **7**(2), 125-147. https://doi.org/10.12989/smm.2020.7.2.125.

Arora, V. (2011), "Comparative study of finite element model updating methods", *J. Vib. Control*, **17**(13), 2023-2039. https://doi.org/10.1177/1077546310395967.

Barbosh, M., Singh, P. and Sadhu, A. (2020), "Empirical mode decomposition and its variants: A review with applications in structural health monitoring", *Smart Mater. Struct.*, **29**(9), 093001. https://orcid.org/0000-0001-5685-7087.

Bayat, M., Ahmadi, H.R. and Mahdavi, N. (2019), "Application of power spectral density function for damage diagnosis of bridge piers", *Struct. Eng. Mech.*, **71**(1), 57-63. https://doi.org/10.12989/sem.2019.71.1.057.

Bendat, J.S. and Piersol, A.G. (1980), *Engineering Applications of Correlation and Spectral Analysis*, New York.

Carbonell, A., González-Vidosa, F. and Yepes, V. (2011), "Design of reinforced concrete road vaults by heuristic optimization", *Adv. Eng. Softw.*, **42**(4), 151-159. https://doi.org/10.1016/j.advengsoft.2011.01.002.

Crank, J. (2004), *The Mathematics of Diffusion-Appendix A Solution of Fick's Second Law*, Oxford University Press, Oxford, UK.

Dessi, D. and Camerlengo, G. (2015), "Damage identification techniques via modal curvature analysis: Overview and comparison", *Mech. Syst. Signal Pr.*, **52**, 181-205. https://doi.org/10.1016/j.ymssp.2014.05.031.

Ekolu, S.O. (2020), "Model for natural carbonation prediction (NCP): Practical application worldwide to real life functioning concrete structures", *Eng. Struct.*, **224**, 111126. https://doi.org/10.1016/j.engstruct.2020.111126.

Esfandiari, A., Bakhtiari-Nejad, F., Rahai, A. and Sanayei, M. (2009), "Structural model updating using frequency response function and quasi-linear sensitivity equation", *J. Sound Vib.*, **326**(3-5), 557-573. https://doi.org/10.1016/j.jsv.2009.07.001.

Ganguli, R. (2020), *Modal Curvature Based Damage Detection. In Structural Health Monitoring*, Springer, Singapore.

Gao, D.Y., Yao, W.X., Wen, W.D. and Huang, J. (2021), "Equivalent spectral method to estimate the fatigue life of composite laminates under random vibration loadings", *Mech. Compos. Mater.*, **57**(1), 101-114. https://doi.org/10.1007/s11029-021-09937-2.

García-Segura, T., Penadés-Plà, V. and Yepes, V. (2018), "Sustainable bridge design by metamodel-assisted multi-objective optimization and decision-making under uncertainty", *J. Clean. Prod.*, **202**, 904-915. https://doi.org/10.1016/j.jclepro.2018.08.177.

González, J.L., Aguilera, F.P. and García, F.R. (2013), "Proyecto de rehabilitación del puente de la Isla de Arosa", *Hormig. Acero.*, **270**, 75-89.

Goyal, A., Pouya, H.S., Ganjian, E. and Claisse, P. (2018), "A review of corrosion and protection of steel in concrete", *Arab. J. Sci. Eng.*, **43**(10), 5035-5055. https://doi.org/10.1007/s13369-018-3303-2.

Gunawan, F.E. (2019), "Reliability of the power spectral density method in predicting structural integrity", *Int. J. Innov. Comput., Inform. Control*, **15**(5), 1717-1727. https://doi.org/10.24507/ijicic.15.05.1717.

Hadizadeh-Bazaz, M., Navarro, I.J and Yepes, V. (2022), "Performance comparison of structural damage detection methods based on frequency response function and power spectral density", *DYNA Ingeniería e Industria*, **97**(5), 493-500. https://doi.org/10.6036/10504.

Hájková, K., Šmilauer, V., Jendele, L. and Červenka, J. (2018), "Prediction of reinforcement corrosion due to chloride ingress and its effects on serviceability", *Eng. Struct.*, **174**, 768-777. https://doi.org/10.1016/j.engstruct.2018.08.006.

Hou, L., Peng, Y., Xu, R., Zhang, X., Huang, T. and Chen, D. (2021), "Corrosion behavior and flexural performance of reinforced SFRC beams under sustained loading and chloride attack", *Eng. Struct.*, **242**, 112553. https://doi.org/10.1016/j.engstruct.2021.112553.

Hou, R., Xia, Y. and Zhou, X. (2018), "Structural damage detection based on l1 regularization using natural frequencies and mode shapes", *Struct Control Hlth. Monit.*, **25**(3), e2107. https://doi.org/10.1002/stc.2107.

Khan, M.U., Ahmad, S. and Al-Gahtani, H.J. (2017), "Chloride-induced corrosion of steel in concrete: An overview on chloride diffusion and prediction of corrosion initiation time", *Int. J. Corros*, **2017**, Article ID 5819202. https://doi.org/10.1155/2017/5819202.

Khan, M.W., Akmal Din, N. and Ul Haq, R. (2020), "Damage detection in a fixed-fixed beam using natural frequency changes", *Vibroeng. Procedia*, **30**, 38-43. https://doi.org/10.21595/vp.2019.21081.

Khosravan, A., Asgarian, B. and Shokrgozar, H.R. (2021), "Improved modal strain energy decomposition method for damage detection of offshore platforms using data of sensors above the water level", *Ocean. Eng.*, **219**, 108337. https://doi.org/10.1016/j.oceaneng.2020.108337.

Li, J.T., Zhu, X.Q. and Samali, B. (2020), "Bridge operational modal identification using sparse blind source separation", *ACMSM25*, Springer, Singapore.

Najafabadi, A.A., Daneshjoo, F. and Bayat, M. (2017), "A novel index for damage detection of deck and dynamic behavior of horizontally curved bridges under moving load", *J. Vibroeng.*, **19**(7), 5421-5433. https://doi.org/10.21595/jve.2017.19370.

Navarro, I.J., Marti, J.V. and Yepes, V. (2019), "Reliability-based maintenance optimization of corrosion preventive designs under a life cycle perspective", *Environ. Impact. Assess. Rev.*, **74**, 23-34. https://doi.org/10.1016/j.eiar.2018.10.001.

Navarro, I.J., Yepes, V. and Martí, J.V. (2018a), "Life cycle cost assessment of preventive strategies applied to prestressed concrete bridges exposed to chlorides", *Sustain.*, **10**(3), 845. https://doi.org/10.3390/su10030845.

Navarro, I.J., Yepes, V. and Martí, J.V. (2018b), "Social life cycle assessment of concrete bridge decks exposed to aggressive environments", *Environ. Impact. Assess. Rev.*, **72**, 50-63. https://doi.org/10.1016/j.eiar.2018.05.003.

Navarro, I.J., Yepes, V., Martí, J.V. and González-Vidosa, F. (2018c), "Life cycle impact assessment of corrosion preventive designs applied to prestressed concrete bridge decks", *J. Clean. Prod.*, **196**, 698-713. https://doi.org/10.1016/j.jclepro.2018.06.110.

Nilsson, A. and Liu, B. (2015), "Frequency domain", *Vibro-Acoust.*, **1**, 31-66. https://doi.org/10.1007/978-3-662-47934-6.

Niu, Z. (2020), "Frequency response-based structural damage detection using Gibbs sampler", *J. Sound Vib.*, **470**, 115160. https://doi.org/10.1016/j.jsv.2019.115160.

Pedram, M., Esfandiari, A. and Khedmati, M. R. (2017), "Damage detection by a FE model updating method using power spectral density: Numerical and experimental investigation", *J. Sound Vib.*, **397**, 51-76. https://doi.org/10.1016/j.jsv.2017.02.052.

Penadés-Plà, V., García-Segura, T. and Yepes, V. (2019), "Accelerated optimization method for low-embodied energy concrete box-girder bridge design", *Eng. Struct.*, **179**, 556-565. https://doi.org/10.1016/j.engstruct.2018.11.015.

Pérez, M.A., Font-Moré, J. and Fernández-Esmerats, J. (2021), "Structural damage assessment in lattice towers based on a novel frequency domain-based correlation approach", *Eng. Struct.*, **226**, 111329. https://doi.org/10.1016/j.engstruct.2020.111329.

Pérez-Fadón Martínez, S. (1985), "Puente a la Isla de Arosa", *Hormigón y Acero*, **36**(157).

Pérez-Fadón Martínez., S (1986), "Puente sobre la Ría de Arosa", *Rev Obras Publicas,* 1-16.

Pooya, S.M.H. and Massumi, A. (2021), "A novel and efficient method for damage detection in beam-like structures solely based on damaged structure data and using mode shape curvature estimation", *Appl. Math. Model.*, **91**, 670-694. https://doi.org/10.1016/j.apm.2020.09.012.

Rahmatalla, S., Eun, H.C. and Lee, E.T. (2012), "Damage detection from the variation of parameter matrices estimated by incomplete FRF data", *Smart Struct. Syst.*, **9**(1), 55-70. https://doi.org/10.12989/sss.2012.9.1.055.

Rathod, H. and Gupta, R. (2019), "Sub-surface simulated damage detection using Non-Destructive Testing Techniques in reinforced-concrete slabs", *Constr. Build. Mater.*, **215**, 754-764. https://doi.org/10.1016/j.conbuildmat.2019.04.223.

Ronchei, C., Vantadori, S., Carpinteri, A., Iturrioz, I., Rodrigues, R.I., Scorza, D. and Zanichelli, A. (2021), "A frequency-domain approach for damage detection in welded structures", *Fatig. Fract. Eng. Mater. Struct.*, **44**(4), 1134-1148. https://doi.org/10.1111/ffe.13419.

Seyedpoor, S.M., Ahmadi, A. and Pahnabi, N. (2019), "Structural damage detection using time domain responses and an optimization method", *Invers. Prob. Sci. Eng.*, **27**(5), 669-688. https://doi.org/10.1080/17415977.2018.1505884.

Shekhar, S., Ghosh, J. and Padgett, J.E. (2018), "Seismic life-cycle cost analysis of ageing highway bridges under chloride exposure conditions: Modelling and recommendations", *Struct. Infrastr. Eng.*, **14**(7), 941-966. https://doi.org/10.1080/15732479.2018.1437639.

Silik, A., Noori, M., Altabey, W.A., Ghiasi, R. and Wu, Z. (2021), "Analytic wavelet selection for time–frequency analysis of big data form civil structure monitoring", *International Workshop on Civil Structural Health Monitoring*, March. https://doi.org/10.1007/978-3-030-74258-4_29.

Sobhani, J. and Ramezanianpour, A.A. (2007), "Chloride-induced corrosion of RC structures", *Asian J. Civil Eng.*, **8**(5), 531-547.

Spanish Ministry of Public Works (2008), EHE-08 Instrucción del Hormigón Estructural.

Sun, B., Xiao, R.C., Ruan, W.D. and Wang, P.B. (2020), "Corrosion-induced cracking fragility of RC bridge with improved concrete carbonation and steel reinforcement corrosion models", *Eng. Struct.*, **208**, 110313. https://doi.org/10.1016/j.engstruct.2020.110313.

Tang, F., Chen, G. and Brow, R.K. (2016), "Chloride-induced corrosion mechanism and rate of enamel-and epoxy-coated deformed steel bars embedded in mortar", *Cement Concrete Res.*, **82**, 58-73. https://doi.org/10.1016/j.cemconres.2015.12.015.

Tran, K.T., Nguyen, T.D., Hiltunen, D.R., Stokoe, K. and Menq, F. (2020), "3D full-waveform inversion in time-frequency domain: Field data application", *J. Appl. Geophy.*, **178**, 104078. https://doi.org/10.1016/j.jappgeo.2020.104078.

Tuutti, K. (1982), "Corrosion of steel in concrete", Cement-och betonginst, Swedish Cement and Concrete Research Institute, Stockholm, Sweden. Report No 4-82.

Wang, Y. (2021), "Adaptive finite element algorithm for damage detection of non-uniform Euler-Bernoulli beams with multiple cracks based on natural frequencies", *Adaptive Analysis of Damage and Fracture in Rock with Multiphysical Fields Coupling* Springer, Singapore.

Wu, Z., Zhang, Z., Wu, J., Liang, J., Ge, J., Liu, X. and Fang, G. (2022), "A new time-frequency domain simulation method for damage accumulation and life prediction of composite thin-wall structures under random cyclic loadings", *Compos. Struct.*, **281**, 114999. https://doi.org/10.1016/j.compstruct.2021.114999.

Xu, W., Zhu, W., Cao, M., Wu, H. and Zhu, R. (2020), "A novel damage index for damage detection and localization of plate-type structures using twist derivatives of laser-measured mode shapes", *J. Sound Vib.*, **481**, 115448. https://doi.org/10.1016/j.jsv.2020.115448.

Yang, Y., Zhang, Y. and Tan, X. (2021), "Review on vibration-based structural health monitoring techniques and technical codes", *Symmetry*, **13**(11), 1998. https://doi.org/10.3390/sym13111998.

Yu, H., Wang, B., Xia, C., Gao, Z. and Li, Y. (2021), "Efficient non-stationary random vibration analysis of vehicle-bridge system based on an improved explicit time-domain method", *Eng. Struct.*, **231**, 111786. https://doi.org/10.1016/j.engstruct.2020.111786.

Zhang, C.L., Chen, W.K., Mu, S., Šavija, B. and Liu, Q.F. (2021), "Numerical investigation of external sulfate attack and its effect on chloride binding and diffusion in concrete", *Constr Build Mater.*, **285**, 122806. https://doi.org/10.1016/j.conbuildmat.2021.122806.

Zhang, D., Zeng, Y., Fang, M. and Jin, W. (2019), "Service life prediction of precast concrete structures exposed to chloride environment", *Adv. Civil Eng.*, **2019**, Article ID 3216328. https://doi.org/10.1155/2019/3216328.

Zheng, X.W., Li, H.N. and Gardoni, P. (2021), "Life-cycle probabilistic seismic risk assessment of high-rise buildings considering carbonation induced deterioration", *Eng. Struct.*, **231**, 111752. https://doi.org/10.1016/j.engstruct.2020.111752.

Zheng, Z.D., Lu, Z.R., Chen, W.H. and Liu, J.K. (2015), "Structural damage identification based on power spectral density sensitivity analysis of dynamic responses", *Comput. Struct.*, **146**, 176-184. https://doi.org/10.1016/j.compstruc.2014.10.011.

CC